A: Environmental, Combustion, and Atmospheric Chemistry; Aerosol Processes, Geochemistry, and Astrochemistry

Reaction Energetics and ^{13}C Fractionation of Alanine Transamination in the Aqueous and Gas Phases

Ashley S. McNeill, Brooke H Dallas, John M Eiler, Eric J. Bylaska, and David A Dixon

J. Phys. Chem. A, **Just Accepted Manuscript** • Publication Date (Web): 30 Jan 2020

Reaction Energetics and ^{13}C Fractionation of Alanine Transamination in the Aqueous and Gas Phases

Ashley S. McNeill,[1] Brooke H. Dallas,[2] John M. Eiler,[2] Eric J. Bylaska,[3] and David A. Dixon[1,*,†]

[1] Department of Chemistry and Biochemistry, The University of Alabama, Tuscaloosa, AL, USA

[2] Division of Geological and Planetary Science, California Institute of Technology, Pasadena, CA, USA

[3] Environmental Molecular Sciences Laboratory, Pacific Northwest National Laboratory, Richland, WA, USA

Abstract

The alanine transaminase (ALT) enzyme catalyzes the transfer of an amino group from alanine to α-ketoglutarate to produce pyruvate and glutamate. Isotope fractionation factors (IFFs) for the reaction $^{+}H_3NCH(CH_3)COO^{-}$ + $^{-}OOCCH_2CH_2C(O)COO^{-}$ ↔ $CH_3C(O)COO^{-}$ + $^{+}H_3NCH(CH_2CH_2COO^{-})COO^{-}$ (zwitterionic neutral alanine + doubly deprotonated α-ketoglutarate ↔ pyruvate + zwitterionic glutamate anion) were calculated from the partition functions of explicitly and implicitly solvated molecules at 298 K. Calculations were done for alanine (non-charge separated, zwitterion, deprotonated,), pyruvic acid (neutral, deprotonated), glutamic acid (non-charge separated, zwitterion, deprotonated, doubly deprotonated), and α-ketoglutaric acid (neutral, deprotonated, doubly deprotonated). The computational results, calculated from gas phase and aqueous optimized clusters with explicit H_2O molecules at the

† Email: dadixon@ua.edu

MP2/aug-cc-pVDZ and MP2/aug-cc-pVDZ/COSMO levels, respectively, predict that substitution of ^{13}C at the C2 position of alanine and pyruvic acid and their various forms leads to the C2 position of pyruvic acid/pyruvate being enriched in $^{13}C/^{12}C$ ratio by 9 ‰. Simpler approaches that estimate the IFFs based solely on changes in the zero-point energies (ZPEs) are consistent with the higher-level model. ZPE-based IFFs calculated for simple analogues formaldehyde and methylamine (analogous to the C2 positions of pyruvate and alanine, respectively) predict a ^{13}C enrichment in formaldehyde of 7 to 8 ‰ at the MP2/aug-cc-pVDZ and aug-cc-pVTZ levels. A simple predictive model using canonical functional group frequencies and reduced masses for ^{13}C exchange between $R_2C=O$ and $R_2CH\text{-}NH_2$ predicted enrichment in $R_2C=O$ that is too large by a factor of two, but is qualitatively accurate compared with the more sophisticated models. Our models are all in agreement with the expectation that pyruvate and formaldehyde will be preferentially enriched in ^{13}C due to the strength of their >C=O bond relative to that of the ≡C-NH_2 in alanine and methylamine. $^{13}C/^{12}C$ substitution is also modeled at the methyl and carboxylic acid sites of alanine and pyruvic acid.

Introduction

The alanine transaminase (ALT) enzyme, which can be found in plasma and other tissues but is most common in the liver, was first characterized in 1955.[1] ALT activity is commonly included in clinical liver function tests as a significantly increased level of ALT is an indicator of liver disease.[2] ALT activity is also influenced by other various factors including drug consumption, viral hepatitis, and metabolic abnormalities.[3] The ALT enzyme catalyzes the reversible transfer of an amino group from alanine to α-ketoglutarate to produce pyruvate and glutamate. An equilibrium isotopic fractionation is expected for the isotope exchange reaction between alanine ($H_2NCH(CH_3)COOH$) and pyruvate ($CH_3C(O)COOH$) with pyruvate preferentially enriched in ^{13}C because the force constant at the >C=O bond minimum is larger than that of ≡C-NH_2.[4]

Experimental studies of the ALT reaction found that the equilibrium constant of the reaction is 0.66 (taken from the experimental value of 1.52 for the reverse reaction) at 25 °C and biological pH (7.4), with experimental variation of less than 9%.[5] Additional experiments with racemic mixtures of alanine and glutamate rather than pure L-alanine and L-glutamate resulted in no change in the overall equilibrium of this reaction. Equilibrium constant values of 0.62 and 0.59 (again taken from the reverse reaction) have been reported for the reaction at biological temperature, 37 °C.[6,7,8] The free energy of the ALT reaction can be obtained from the K_{eq} values and is close to zero, 1.04 ± 0.13 kJ/mol (0.25 kcal/mol).[8]

In this work, we predict the equilibrium isotope fractionation factor (IFF) for the reversible ALT reaction at a variety of computational levels. Additionally, $^{13}C/^{12}C$ substitution of alanine and pyruvic acid at the methyl and carboxylic acid sites, unrelated to the ALT reaction, are also modeled.

Computational Details

The Car-Parrinello simulations[9] in this study were performed using an *ab initio* molecular dynamics approach (AIMD) and a combined ab initio and classical molecular dynamics (AIMD/MM) approach that is part of the pseudopotential plane-wave program (NWPW module) contained in the NWChem quantum chemistry package.[10] This method couples the pseudopotential plane-wave solvers[11,12] of the Density Functional Theory (DFT) equations[13,14] for the quantum mechanics region to a molecular mechanics description of a larger region. In the AIMD/MM method the total energy for the system is given by a sum of E_{AIMD}, E_{MM}, and $E_{AIMD/MM}$,where E_{AIMD} and E_{MM} are energies for quantum mechanics and molecular mechanics regions, respectively. Details about the method can be found in Cauet et al.[15] The PBE96[16] gradient corrected exchange-correlation functional was used. The valence electron interactions with the atomic H, C, N and O cores were approximated using generalized norm-conserving Hamann pseudopotentials[17,18] modified into a separable form as suggested by Kleinman and Bylander.[19] The original pseudopotential parameterizations suggested by Hamann[18] were too 'hard,' and softer pseudopotentials were constructed by increasing the core radii giving: H: r_{cs} = 0.8 au, r_{cp} = 0.8 au; C: r_{cs} = 0.8 au, r_{cp} = 0.85 au, r_{cd} = 0.85 au; N: r_{cs} = 0.7 au, r_{cp} = 0.7 au, r_{cd} = 0.7 au; O: r_{cs} = 0.7 au, r_{cp} = 0.7 au, r_{cd} = 0.7 au. The electronic wavefunctions were expanded using a plane-wave basis set with periodic boundary conditions, sampled at the Γ point, with a wavefunction cutoff energy of 100 Ry and a density cutoff energy of 200 Ry. A homogeneous negative charge background neutralized the −1 charge used in these simulations. The Car-Parrinello equations of motion[9] were integrated in the presence of Nose-Hoover thermostats,[20,21,22] coupled to the electronic and ionic degrees of freedom, at T = 300 K with a time step of 0.17 fs and a fictitious mass of 750 au. The simulation cells were simple cubic. They were chosen to have a concentration of 1 M (i.e. solute

+ 56 H_2O) and 0.5 M (i.e. solute + 112 H_2O) with a density of water near 1. A Shrake-Rupley algorithm[23] was used to determine the volumes of the amino acid solute. The SPC/E MM potential for water was used in the QM/MM portion of this study.[24] The parameters for this potential and the QM/MM potential used in this work are given in the Supporting Information. EMSL Arrows[25] was used generate the input decks and perform these calculations.

In order to model the overall reactions of interest, shown in Figure 1, the structures of molecules with single solvation shells of explicit H_2O molecules for each of the four anions were isolated from the AIMD and AIMD/MM simulations; these starting structures are shown in Figure S1. This protocol is rationalized in terms of Inherent Structure Theory[26] in which a thermal ensemble of atomic configurations is mapped (by steepest descent) onto potential energy minima, to produce an ensemble averaged IFF. This type of sampling strategy allows for averaging over multiple solvent configurations, while at the same time only having to compute explicit IFFs on a small number of samples. Protons were added to the anions to form neutral species for all four molecules, which for alanine and glutamic acid includes non-charge separated (NCS) and zwitterionic structures. There are two versions of the glutamic acid zwitterion, one with the negative charge on the C-terminus and one with the negative charge on the side chain carboxylate. A variation of the glutamate anion structure with a zwitterionic backbone was also modeled in which the N-terminus has an additional proton and both carboxylates are deprotonated. Protons were removed to generate the glutamate and α-ketoglutarate dianions. For glutamate, a second anionic structure was generated by moving the proton from the side chain carboxylic acid group to the C-terminus carboxylic acid group. For α-ketoglutarate, a second anion was generated by moving the proton from the carboxylic acid of glutarate moiety to the carboxylate of the α-keto moiety (Figure 2). These initial structures were optimized at the density functional theory (DFT)

level using the hybrid exchange-correlation method B3LYP[27,28] with the DZVP2[29] basis set. Any explicit H_2O molecules that left the first solvation shell were removed before the next iteration of optimization for all neutral and ionic species. The number of H_2O molecules in the variations of a given chemical species with the largest first solvation shell was maintained for all other variations of that molecule. This results in species with additional H_2O molecules not contained in the first solvation shell for our simulations, but those additional H_2O molecules do not affect the energetics of the overall reaction.

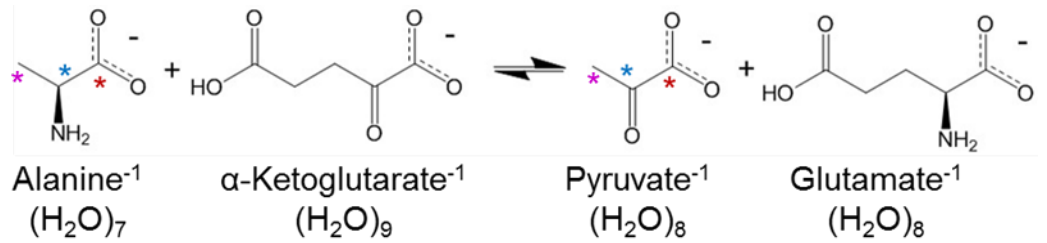

(1)

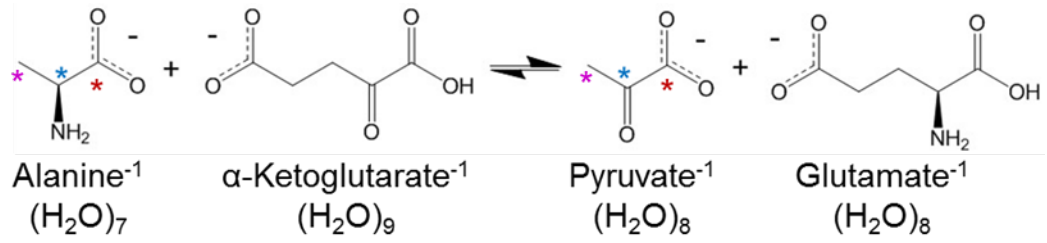

(2)

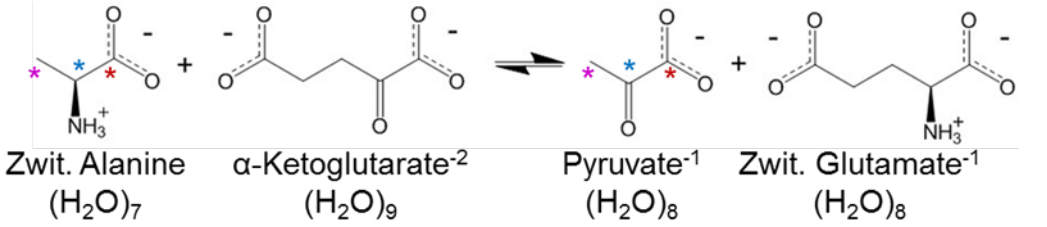

(3)

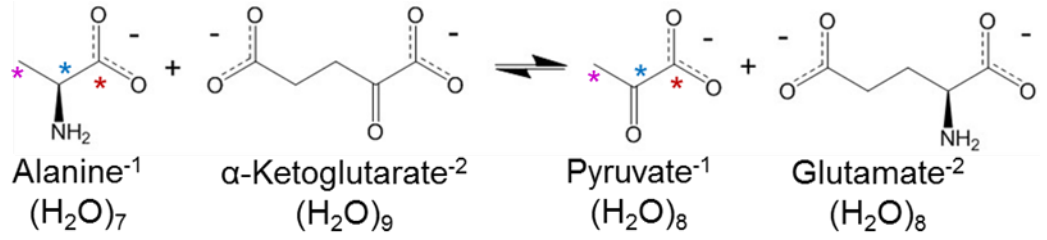

(4)

Figure 1. Reaction (1) is that for the alanine anion and α-ketoglutarate deprotonated at the α-keto moiety (-C(O)C(O)O^-) forming pyruvate and glutamate deprotonated at the C-terminus. Reaction

(2) has α-ketoglutarate deprotonated at the glutarate moiety ($-CH_2C(O)O^-$) and glutamate deprotonated at the side chain. Reaction (3) represents each chemical species as it would be present at biological pH. Reaction (4) has all carboxylate groups deprotonated for all species. H_2O molecules not shown for clarity. Red, blue, and purple asterisks (*) indicate sites of ^{13}C substitution at the carboxylate group, the C2 position, and the methyl group, respectively.

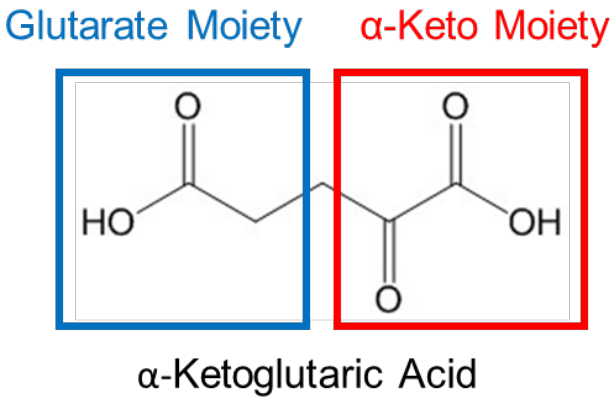

Figure 2. Carboxylic acid deprotonation sites for α-ketoglutaric acid. The glutarate moiety is analogous to the side chain of glutamic acid and the α-keto moiety is analogous to the C-terminus of glutamic acid.

The B3LYP/DZVP2-optimized geometries were reoptimized at the correlated molecular orbital (MO) theory MP2 level[30,31] with the aug-cc-pVDZ (aD) basis set[32,33] in the gas phase and in the presence of implicit aqueous solvation using a self-consistent reaction field (SCRF) approach[34] with COSMO[35,36] parameters. The MP2 level was chosen because we need to be able to calculate vibrational frequencies and due to issues with non-bonding interactions with most density functional theory exchange-correlation functionals. Such geometry optimizations and frequency calculations are not feasible computationally with higher levels of correlated molecular orbital theory. In addition, the MP2 method provides excellent energetics for hydrogen bonding

for water molecules[37] and has been shown to provide good isotope fractionation factors in aqueous and mineral carbonates.[38] For the gas phase optimized structures, aqueous corrections were also calculated at the MP2/aD/COSMO level and aqueous free energies (ΔG_{aq}) were calculated according to Equation (5).

$$\Delta G_{aq} = \Delta G_{gas} + \Delta G_{solv} \quad (5)$$

A dielectric constant of 78.39 corresponding to that of bulk water was used in the COSMO calculations. The solvation energy includes only the electrostatic energy component. Gas phase optimized geometries were also reoptimized in aqueous solution at the MP2/aD/COSMO level. All calculations were performed using the Gaussian 16 software package.[39] Harmonic vibrational frequencies were calculated for MP2/aD and MP2/aD/COSMO optimized clusters for use in the isotopic fractionation calculations.

The calculated vibrational frequencies for "light" (all isotopically light atoms: ^{1}H, ^{12}C, ^{14}N, ^{16}O) and "heavy" (one ^{13}C with all otherwise isotopically light atoms) isotopes were used to calculate isotopic fractionation ratios for $^{13}C/^{12}C$ at the C2 site and the carboxylic acid and methyl groups for alanine and pyruvic acid. The vibrational partition functions (relative to the minimum of the potential energy surface) for a given cluster, q_{vib}, were calculated using Equation (6)

$$q_{vib,i} = \frac{e^{-\Theta_i/2T}}{1-e^{-\Theta_i/T}} \quad (6)$$

where $\Theta_i = h\upsilon_i/k_B$ and υ_i are the individual fundamental modes for a given species as calculated at the MP2/aD or MP2/aD/COSMO level. The individual vibrational partition functions are then used to calculate Q for each cluster, (Equation (7)).

$$Q = \prod_i \frac{\theta_i}{T} q_{vib,i} = \prod_i \frac{\theta_i}{T} \frac{e^{-\Theta_i/2T}}{1-e^{-\Theta_i/T}} \quad (7)$$

We use the vibrational partition functions of each compound to evaluate the equilibrium constants for reactions shown in Figure 1, both for the versions of those reactions involving reactants and

products containing ^{12}C in all carbon positions (indicated with the subscript 'l' to signify isotopically light) and for versions that contain a ^{13}C in one of the carbon positions of reactant alanine and product pyruvate (indicated with the subscript 'h' to signify isotopically heavy). This results in two related equations for the equilibrium constant for each reaction — K_l for the reaction involving only isotopically light reactants and K_h for the reaction involving one isotopically heavy reactant and product. Equations (8) and (9) illustrate this nomenclature.

$$K_l = \frac{Q_{Pyr,l}Q_{Glu,l}}{Q_{Ala,l}Q_{\alpha-Ket,l}} \quad (8)$$

$$K_h = \frac{Q_{Pyr,h}Q_{Glu,l}}{Q_{Ala,h}Q_{\alpha-Ket,l}} \quad (9)$$

The isotope fractionation factor (IFF; ϵ) associated with the reaction is determined by taking the ratio of the equilibrium constant for the version of the reaction having heavy isotopes to the equilibrium constant for the version of the reaction with all light isotopes. This value is calculated as shown in Equation (10).

$$\epsilon = \left[\left(\frac{K_h}{K_l}\right) - 1\right] * 1000 \quad (10)$$

We also use the vibrational frequencies of isotopically heavy and light forms of the studied compounds to calculate the reduced partition function ratios (RPFR; β), which provide a measure of the propensity of a compound of interest to concentrate a heavy isotope relative to a pool of free atoms of the relevant element. Comparison of β values for two compounds provides a measure of the tendency of heavy isotopes to partition into one vs. the other compound at equilibrium. Similarly, when β values are computed for two different isotopomers of the same compound, comparison of these values indicates whether the heavy isotope of interest preferentially concentrates in one vs. the other atomic site. Values of β were calculated in the harmonic approximation for each individual species as shown in Equation (11)

$$\beta = \frac{Q_h}{Q_l} = \frac{\prod_i \theta_i q_{vib,h,i}}{\prod_j \theta_j q_{vib,l,j}} \quad (11)$$

where Q_h is the Q value of the isotope that contains a ^{13}C at a given site and Q_l is the Q value of the isotope with only ^{12}C atoms.

Equilibrium constants are also calculated from the free energies in the gas phase and in aqueous solution and are given as K′. These are determined using the standard thermodynamic relationship in Equation (12).

$$K' = e^{-\Delta G/RT} \quad (12)$$

Or, equivalently, lnK' = -ΔG/RT. This approach can also be used to estimate the IFF associated with a reaction by approximating ΔG values with zero-point energies of reaction (reaction at 0 K). Specifically, we can estimate the IFF as ϵ_{ZPE} = 1000*lnK_{ZPE}, where lnK_{ZPE} is computed as shown in Equation (13)

$$lnK_{ZPE} = \frac{-\Delta\Delta ZPE}{RT} \quad (13)$$

where ΔΔZPE is the difference between ΔZPE values for the heavy isotope-containing molecules in an isotope fractionation equilibrium, which are calculated as follows in equation (14), in which ω_i^{12} and ω_i^{13} are fundamental frequencies with all isotopically light atoms or with one substituted ^{13}C atom, respectively.

$$\Delta ZPE = \sum_i \frac{1}{2} hc(\omega_i^{12} - \omega_i^{13}) \quad (14)$$

A positive ϵ or ϵ_{ZPE} value indicates that the reaction favors formation of the heavy isotope product over heavy isotope reactant in an equilibrium between two species.

Benchmarking was performed for all of the above calculation types by modeling equilibrium isotope fractionation between formaldehyde and methylamine as well as various deprotonated forms of pyruvic acid and alanine with no explicit solvation. Three DFT methods –

B3LYP, LSDA,[13,14,40,41] and BP86[42,43] – using the DZVP2 basis set were compared with values derived from MP2 calculations with the aD and aT (aug-cc-pVTZ)[32,33] basis sets. These values are also compared to similar calculations performed using the NWChem software;[10] the B3LYP, LSDA, and BP86 DFT methods were used with the 6-311++G(2d,2p) basis set[44] in addition to MP2/aT calculations.

Results and Discussion

Optimized Geometries and Deprotonation Energies with Explicit H_2O. Starting from the initial structures taken from the MD simulations (Figure S1), gas phase geometry optimization resulted in final structures for alanine with 7 explicit H_2O molecules, glutamic acid with 8 explicit H_2O molecules, pyruvic acid with 6 explicit H_2O molecules, and α-ketoglutaric acid with 9 explicit H_2O molecules (Figures S2-S6). The inclusion of larger numbers of H_2O molecules resulted in the extra H_2O molecules moving into a second solvent shell. The number of explicit H_2O molecules were kept consistent despite the structure of or charge on the molecule of interest to compare the energies of the resulting optimized geometries directly. These gas phase optimized geometries were reoptimized in aqueous solution at the MP2/aD/COSMO level are also given in Figures S2-S6. The reactions of interest involve the zwitterionic structures of alanine and glutamic acid as well as deprotonated forms of the amino acids, pyruvic acid, and α-ketoglutaric acid.

Gas phase and aqueous free energies for the formation of the various species for alanine, glutamic acid, pyruvic acid, and α-ketoglutaric acid and their deprotonated forms are summarized in Table 1. When reoptimized in aqueous solution, the molecules of interest do not differ in geometry, but the explicit H_2O molecules in each cluster can reorganize in the single solvation shell and may leave the first solvent shell. This can result in differences between gas phase optimized ΔG_{aq} and aqueous optimized ΔG_{aq}. The calculated pK_a values for deprotonation of

aqueous optimized clusters are systematically higher by 1 to 8 pK_a units with respect to deprotonation of gas optimized clusters. All the discussion is based on the organic molecules in their cluster of H_2O solvent molecules. These calculated pK_a values are compared to experimental values[45] in Table 1 and are discussed below.

For alanine (Figure S2), the formation of the zwitterion is exergonic and favorable in both the gas phase and aqueous optimized clusters by -15.3 and -10.5 kcal/mol respectively at the MP2/aD/COSMO level. This is expected for an amino acid in aqueous solution. The aqueous free energy of the deprotonation of alanine is -6.7 kcal/mol for the gas phase optimized reaction and 4.1 kcal/mol for the aqueous optimized structure. However, in aqueous solution alanine is present as a zwitterion rather than a structure without charge separation. Aqueous deprotonation of zwitterionic alanine is endergonic for both gas and aqueous optimized clusters by 8.6 and 14.6 kcal/mol respectively at the MP2/aD/COSMO level. The gas phase and aqueous optimized pK_a values for neutral zwitterionic alanine losing a proton to form anionic alanine are 6.3 and 10.7, as compared to an experimental value of 9.87.[45] In this case, the optimized aqueous phase structure yields a pK_a closer to experiment. The use of the gas phase structures, except in the case of formation of the glutamate dianion, give pK_a values that are too acidic.

For glutamic acid (Figure S3), the gas phase and aqueous optimized modeled reactions are endergonic. Deprotonation of glutamic acid was modeled at the C-terminus, the side chain carboxylic acid, or with double deprotonation at both carboxylic acid groups. Deprotonation at the C-terminus of glutamic acid yields an aqueous reaction free energy of 6.7 and 14.2 kcal/mol for the gas and aqueous optimized reactions respectively at the MP2/aD/COSMO level. Deprotonation at the side chain of glutamic acid is more favorable than at the C-terminus with aqueous free energies of 0.8 kcal/mol for the gas phase optimized reaction and 12.1 kcal/mol for the aqueous

Table 1. Gas Phase and Aqueous Free Energy Values for Various Reactions at the MP2/aD and MP2/aD/COSMO Levels at 298 K in kcal/mol.

Reaction	# of H_2O Molecules [a]	ΔG_{gas}	$\Delta G_{aq,\ gas\ opt}$	$\Delta G_{aq,\ aq\ opt}$	Calc. Gas Opt pK_a	Calc. Aq Opt pK_a	Expt pK_a [b]
Alanine → Alanine Zwitterion	7	-5.6	-15.3	-10.5			
Alanine → Deprotonated Alanine + H^+	7	299.2	-6.7	4.1	-4.9	3.0	
Protonated Alanine → Alanine + H^+	7	236.9	17.6	20.3	12.9	14.9	
Alanine Zwitterion → Deprotonated Alanine + H^+	7	304.8	8.6	14.6	6.3	10.7	9.87
Protonated Alanine → Alanine Zwitterion + H^+	7	231.3	2.3	9.8	1.7	7.2	2.34
Glutamic Acid → Glutamate (C-terminus Deprotonation) + H^+	8	297.3	6.7	14.2	4.9	10.4	
Glutamic Acid → Glutamate (Side Chain Deprotonation) + H^+	8	297.9	0.8	12.1	0.6	8.8	
Glutamic Acid → Glutamate (Doubly Deprotonated) + $2H^+$	8	661.3	10.1	22.5			
Glutamic Acid Zwitterion (C-terminus) → Zwitterionic Glutamate Anion + H^+	8	294.6	2.4	12.5	1.7	9.2	4.31
Zwitterionic Glutamate Anion → Glutamate (Doubly Deprotonated) + H^+	8	359.5	15.0	16.4	11.0	12.0	9.67
Pyruvic Acid → Pyruvate + H^+	6	295.7	0.5	5.4	0.4	4.0	2.39
α-Ketoglutaric Acid → α-Ketoglutarate ($-C(O)C(O)O^-$) + H^+	9	286.7	-4.0	2.2	-3.0	1.6	2.47
α-Ketoglutaric Acid → α-Ketoglutarate ($-CH_2C(O)O^-$) + H^+	9	283.5	-2.4	6.1	-1.8	4.5	2.47
α-Ketoglutarate ($-C(O)C(O)O^-$) → Doubly Deprotonated α-Ketoglutarate + $2H^+$	9	354.4	2.4	8.4	1.8	6.2	4.68

[a] Number of H_2O molecules indicates the total number of explicit H_2O molecules included in all gas phase and aqueous geometry optimizations for all species present in the given reactions. [b] Ref. 45.

phase optimized reaction. Thus, deprotonation at the C-terminus is 5.9 kcal/mol and 2.1 kcal/mol higher in aqueous free energy than deprotonation at the side chain of glutamic acid for the gas phase and aqueous phase optimized reactions, respectively. Aqueous deprotonation of both carboxylic acid sites requires 22.5 kcal/mol for the gas phase and aqueous optimized reactions. The deprotonation of the side chain following the first deprotonation at the C-terminus requires an aqueous free energy change of 9.3 and 10.4 kcal/mol for the gas phase and aqueous optimized reactions, respectively.

In aqueous solution, the zwitterionic glutamic acid structure is preferred. For the gas phase optimized clusters, the NCS glutamic acid with 8 explicit H_2O molecules is favored over the zwitterionic glutamic acid structures. Compared to the $\Delta G_{gas,298K}$ of NCS glutamic acid, zwitterionic glutamic acid with the C-terminus deprotonated is 7.3 kcal/mol higher and zwitterionic glutamic acid with the side chain deprotonated is 3.4 kcal/mol higher in free energy at 298 K. For the aqueous optimized clusters, the zwitterionic glutamic acid with deprotonated C-terminus is lowest in free energy at 298 K, with relative $\Delta G_{aq,298K}$ values for the zwitterionic glutamic acid with deprotonation at the side chain of 2.6 kcal/mol and for NCS glutamic acid of 6.4 kcal/mol. Aqueous glutamate anions also exists with a zwitterionic backbone. In the gas phase, the $\Delta G_{gas,298K}$ of the glutamate zwitterion is 4.0 kcal/mol higher than the glutamate structure with the side chain deprotonated and a NCS backbone, but the glutamate zwitterion is 5.7 kcal/mol more favorable than the side chain anion with the NCS backbone in $\Delta G_{aq,298K}$ for the gas optimized cluster. Similarly, for the aqueous optimized cluster, $\Delta G_{aq,298K}$ is 6.0 kcal/mol higher for the NCS backbone glutamate side chain anion than for the zwitterionic glutamate anion. Zwitterionic glutamic acid deprotonation reactions compared to experimental pK_a's for aqueous glutamic acid are shown in Figure S4. The gas phase and aqueous optimized pK_a values for neutral zwitterionic

glutamic acid losing a proton to form the zwitterionic glutamate anion are 1.7 and 9.2, which can be compared to the experimental pK_a of 4.31.[45] Again, the gas phase optimized structure pK_a is in better agreement with experiment. The gas phase and aqueous optimized pK_a values for zwitterionic glutamate anion losing a proton to form dianionic glutamate are 11.0 and 12.0, which can be compared to the experimental value of 9.67.[45] Both calculated values are not acidic enough. Aqueous deprotonation of pyruvic acid to form pyruvate is very slightly endergonic for the gas phase optimized reaction (0.5 kcal/mol) and endergonic for the aqueous optimized reaction (5.4 kcal/mol), as shown in Figure S5. The gas phase and aqueous optimized pK_a values for pyruvic acid losing a proton to form pyruvate are 0.4 and 4.0, which can be compared to an experimental pK_a of 2.39.[45] Both calculated values are in good agreement with experiment.

For α-ketoglutaric acid (Figure S6), reactions between gas phase optimized structures are exergonic and those between aqueous optimized structures are endergonic. Deprotonation of α-ketoglutaric acid was modeled at either the -C(O)C(O)OH (α-keto moiety), which is analogous to the C-terminus of an amino acid, the $-CH_2C(O)OH$ (glutarate moiety), which we consider analogous to the side chain of glutamic acid, or with both carboxylic acid groups deprotonated. The gas phase optimized reaction free energies for formation of these respective deprotonation products are -4.0, -2.4, and -1.6 kcal/mol, respectively. Those for aqueous phase optimized reactions are 2.2, 6.1, and 10.6 kcal/mol, respectively. Regardless of optimization method, deprotonation is preferred at the α-keto moiety ($-C(O)C(O)O^-$) over deprotonation at the glutarate moiety ($-CH_2C(O)O^-$) by 1.6 kcal/mol for the gas optimized reaction and by 3.9 kcal/mol for the aqueous optimized reaction at the MP2/aD/COSMO level. Deprotonation at both carboxylic acid groups on α-ketoglutaric acid is -1.6 kcal/mol for the gas phase optimized reaction and 10.6 kcal/mol for the aqueous phase optimized reaction, which requires an additional 3.4 kcal/mol for

the gas phase optimized reaction and 8.4 kcal/mol for the aqueous phase optimized reaction beyond the deprotonation at the α-keto moiety site. The gas phase and aqueous optimized pK_a values for α-ketoglutaric acid losing a proton to form the lowest energy anion (deprotonated at the α-keto moiety) are -3.0 and 1.6, which can be compared to the experimental pK_a of 2.47.[45] Further deprotonation of this anion to form the α-ketoglutarate dianion yields gas phase and aqueous optimized pK_a's of 1.8 and 6.2, which can be compared to the experimental value of 4.68.[45] In this case, the solution optimized structures gives better agreement with experiment for both values.

Transamination Reaction Energetics. The calculated energetics of Reactions (1) through (4), as shown in Figure 1, are given in Table 2 in terms of enthalpy, free energy, and equilibrium constant in the gas phase and the free energy and equilibrium constant in aqueous solution at 298 K for each species with explicit solvation. These values are given for the reactions with all light isotopes. In the gas phase, Reaction (1), which involves α-ketoglutarate deprotonated at the α-keto moiety and glutamate deprotonated at the C-terminus, is both exothermic (ΔH_{gas}(298 K) = -8.8 kcal/mol) and exergonic (ΔG_{gas}(298 K) = -2.9 kcal/mol) at the MP2/aD level. In aqueous

Table 2. Reaction Energies with Explicit H_2O Molecules in the Gas Phase and in Aqueous Solution in kcal/mol with All Light Isotopes.

Energy	Reaction (1)	Reaction (2)	Reaction (3)	Reaction (4)
$\Delta H_{gas,298K}$	-8.8	-2.4	-46.5	7.6
$\Delta G_{gas,298K}$	-2.9	0.9	-47.9	6.8
$\Delta G_{aq,298K}$ Gas Opt	5.8	-1.7	-3.9	6.8
$\Delta G_{aq\ 298K}$ Aq Opt	8.0	2.0	3.8	7.9
$K'_{aq,298K}$ Gas Opt	5.9042×10^{-5}	1.6800×10^{1}	7.2695×10^{2}	1.0402×10^{-5}
$K'_{aq,298K}$ Aq Opt	1.3634×10^{-6}	3.4425×10^{-2}	3.3427×10^{-5}	1.6640×10^{-6}

[a] In each reaction, alanine anion has 7 explicit H_2O molecules, α-ketoglutarate has 9 explicit H_2O molecules, pyruvate has 8 explicit H_2O molecules, and glutamate has 8 explicit H_2O molecules.

solution, both the gas phase and aqueous optimized reactions are endergonic at 5.8 and 8.0 kcal/mol respectively at the MP2/aD/COSMO level. Reaction (2), which involves α-ketoglutarate deprotonated at the glutarate moiety and glutamate deprotonated at the side chain, is exothermic (ΔH_{gas}(298 K) = -2.4 kcal/mol) and slightly endergonic (ΔG_{gas}(298 K) = 0.9 kcal/mol) in the gas phase. Thus, this reaction is less favorable than Reaction (1) by 3.8 kcal/mol (ΔG_{gas}(298 K)) at the MP2/aD level in the gas phase. In aqueous solution, the free energy of Reaction (2) is more favorable than Reaction (1) for the gas phase and aqueous optimized solutions. In aqueous solution, the gas phase optimized free energy is exergonic at -1.7 kcal/mol and is endergonic at 2.0 kcal/mol for the aqueous optimized reaction. These values are 7.5 and 6.0 kcal/mol more favorable than those of Reaction (1) for the gas phase and aqueous optimized reactions, respectively. Reaction (3) contains each species as it would appear at biological pH (7.4) – zwitterionic alanine and doubly deprotonated α-ketoglutarate in equilibrium with deprotonated pyruvate and the zwitterionic glutamate anion structure. This reaction is much more highly exothermic in the gas phase (ΔH_{gas}(298 K) = -46.5 kcal/mol; ΔG_{gas}(298 K) = -47.9 kcal/mol) than any of the other equilibrium reactions between other variations of these species. However, in aqueous solution, both the gas phase and aqueous optimized reactions are comparable in energy to Reaction (2) with gas phase optimized ΔG_{aq}(298 K) = -3.9 kcal/mol and aqueous optimized ΔG_{aq}(298 K) = 3.8 kcal/mol. These calculated values bracket the experimentally determined free energy for the ALT reaction, 0.25 kcal/mol.[8] Considering the difficulty of calculating the aqueous free energy of the dianion accurately with SCRF approaches, both of our ΔG_{aq}(298 K) values are consistent with experiment. Reaction (4), involving doubly deprotonated α-ketoglutarate and glutamate, is endothermic and endergonic in the gas phase and endergonic in aqueous solution. In the gas phase, Reaction (4) has an enthalpy of 7.6 kcal/mol and a free energy of 6.8 kcal/mol at 298 K. In aqueous

solution, both of the gas phase aqueous optimized reactions are nearly as endergonic as the aqueous optimized Reaction (1) at 6.8 and 7.9 kcal/mol, respectively.

Position-Dependent RPFRs for Explicitly Solvated Species. Before describing the predicted IFFs, we describe the results for the Q values. The Q values calculated directly from the frequencies determined at the MP2/aD level for gas phase optimized clusters and the MP2/aD/COSMO level for aqueous phase optimized clusters for both light isotopes (^{12}C only; Q_l) and each heavy isotope (^{13}C at a single carbon site, Q_h) are given in Table S3 in the SI for both the gas phase and aqueous cluster geometries of alanine, glutamic acid, pyruvic acid, and α-ketoglutaric acid as different isomeric and charged (addition or loss of a proton) species with explicit H_2O molecules. These Q values were used to calculate the reduced partition function ratio (RPFR, β) values that are given in Table 3 for the vibrational component only with respect to the site of ^{13}C substitution. The β values indicate whether a given site in the molecule of interest will become enriched in ^{13}C. For all species modeled in both the gas phase and aqueous solution, $\beta > 1$, which indicates that enrichment in ^{13}C at all modeled sites is favorable to varying degrees. Each of the four species of interest and their various forms are modeled with all light isotopes as well as with one carbon replaced with a heavy ^{13}C. Values for β are reported for both gas phase and aqueous optimized clusters of the molecules of interest and their respective explicit H_2O molecules. The gas phase and aqueous optimized β values are very similar for all reported species, so only the aqueous optimized β_{aq} values will be discussed as these most accurately represent the environment of the aqueous species of interest during the ALT reaction. Additionally, we compare to the ^{13}C/^{12}C exchange at other C sites in the alanine and pyruvic acid species, despite the fact that the ALT reaction does not provide pathways for equilibrating some of these families of sites. For example, if you were to ^{13}C label the methyl group of pyruvate, that label would be transferred to the methyl

group of alanine through the ALT chemistry, but it would never migrate into the terminus or C2 sites of either compound.

Table 3. Reduced Partition Function Ratios at Various Carbon Atoms at 298 K.

Species	# of H_2O Molecules	^{13}C Site	$\beta_{gas\ opt}$	$\beta_{aq\ opt}$	$\Delta\beta$ (‰) [a]
Alanine	7	Methyl	1.1434	1.1439	-0.484
		C2	1.1727	1.1736	-0.857
		C-terminus	1.1986	1.1954	3.202
Alanine, Zwitterion	7	Methyl	1.1446	1.1448	-0.276
		C2	1.1731	1.1734	-0.311
		C-terminus	1.1986	1.1941	4.460
Alanine, Deprotonated	7	Methyl	1.1418	1.1413	0.500
		C2	1.1725	1.1733	-0.809
		C-terminus	1.1986	1.1941	4.533
Pyruvic Acid	6	Methyl	1.1416	1.1412	0.316
		C2	1.1836	1.1825	1.101
		Carboxylic Acid	1.1936	1.1904	3.160
Pyruvate	6	Methyl	1.1392	1.1391	0.151
		C2	1.1838	1.1841	-0.297
		Carboxylate	1.1954	1.1934	1.951
Pyruvate	8	Methyl	1.1390	1.1391	-0.129
		C2	1.1828	1.1839	-1.080
		Carboxylate	1.1948	1.1932	1.624

[a] $\Delta\beta$ is calculated as $(\beta_{gas} - \beta_{aq})*1000$.

Figure 3 shows the cumulative β values with vibrational frequency (i.e., cumulative product of the contributions to β from each fundamental mode) for all ^{13}C-substituted forms of alanine (with 7 explicit H_2O molecules) and pyruvic acid (with 6 explicit H_2O molecules). The inclusion of 2 additional explicit H_2O molecules for pyruvate, to make a total of 8 explicit H_2O, did not affect the β values. Sharp increases in β indicate vibrational frequencies that contribute significantly to the reduced partition function ratio when either the methyl, the C2, or the C-terminus site contains a heavy carbon. The cumulative β vs. frequency plots for gas phase and aqueous optimized structures are very similar for alanine-based and pyruvic acid-based species,

showing that different optimization procedures do not greatly affect the cumulative β. For alanine and pyruvic acid with $^{13}C/^{12}C$ substitution at the C2 and methyl sites, neutral and deprotonated species have extremely similar cumulative β plots, regardless of charge or conformation. For all alanine and pyruvic acid species with $^{13}C/^{12}C$ substitution at the methyl group, asymmetric C-H stretches at the methyl sites contribute most significantly to the cumulative β at ~ 3100 to 3200 cm^{-1}. $^{13}C/^{12}C$ substitution for alanine results in a significant contribution at ~ 3100 cm^{-1} from the C-H stretch at the C2 position. Substitution at the C2 site of pyruvic acid, on the other hand, has a significant contribution from the C=O stretch at the C2 site at ~1650 cm^{-1}. However, $^{13}C/^{12}C$ substitution at the carboxylic acid site, the neutral or deprotonated state of the alanine or pyruvic acid molecule affects the frequency that contributes most to the cumulative β. Because the protonated state of the molecule affects the atoms directly bonded to the carboxylic acid/carboxylate, neutral and anionic alanine-based and pyruvic acid-based species have significant contributions to the cumulative β that arise from unique fundamental modes. For NCS neutral alanine, $^{13}C/^{12}C$ substitution at the C-terminus yields a significant contribution to β at ~ 1690 cm^{-1} (C=O asymmetric stretch coupled with the H-O-C bend). For deprotonated alanine, the loss of the H-O bond results in a red-shifted C=O asymmetric stretch coupled with the H-C-C bend that occurs at ~1500 cm^{-1}. For zwitterionic alanine, the NH_3 symmetric bend mode dominates with a small amount of coupling with the C=O asymmetric stretch at the C-terminus (~ 1520 cm^{-1}). For pyruvic acid, there are two significantly contributing fundamental modes, the C=O stretch at the C2 site, and the C=O asymmetric stretch at the carboxylic acid coupled with the H-O-C bend (1690 to 1720 cm^{-1}). $^{13}C/^{12}C$ substitution at the carboxylate for pyruvate, regardless of the number of explicit H_2O molecules, has a significant contribution at 1535 cm^{-1} from the C=O asymmetric stretch mode coupled with one or more H-O-H bends from the explicit H_2O molecules.

Substitution of ^{13}C into carbon sites of glutamic acid and α-ketoglutaric acid species are not relevant to Reactions (1) through (4), so discussion of these β values is in the SI.

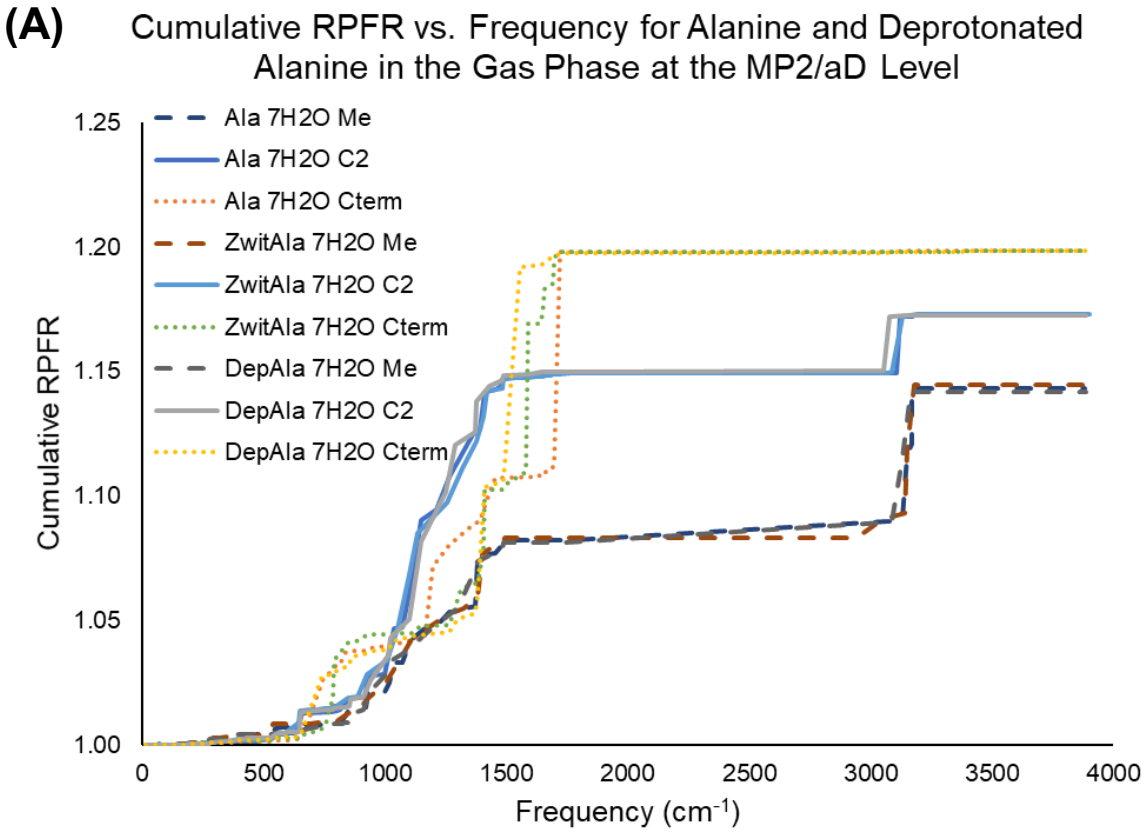

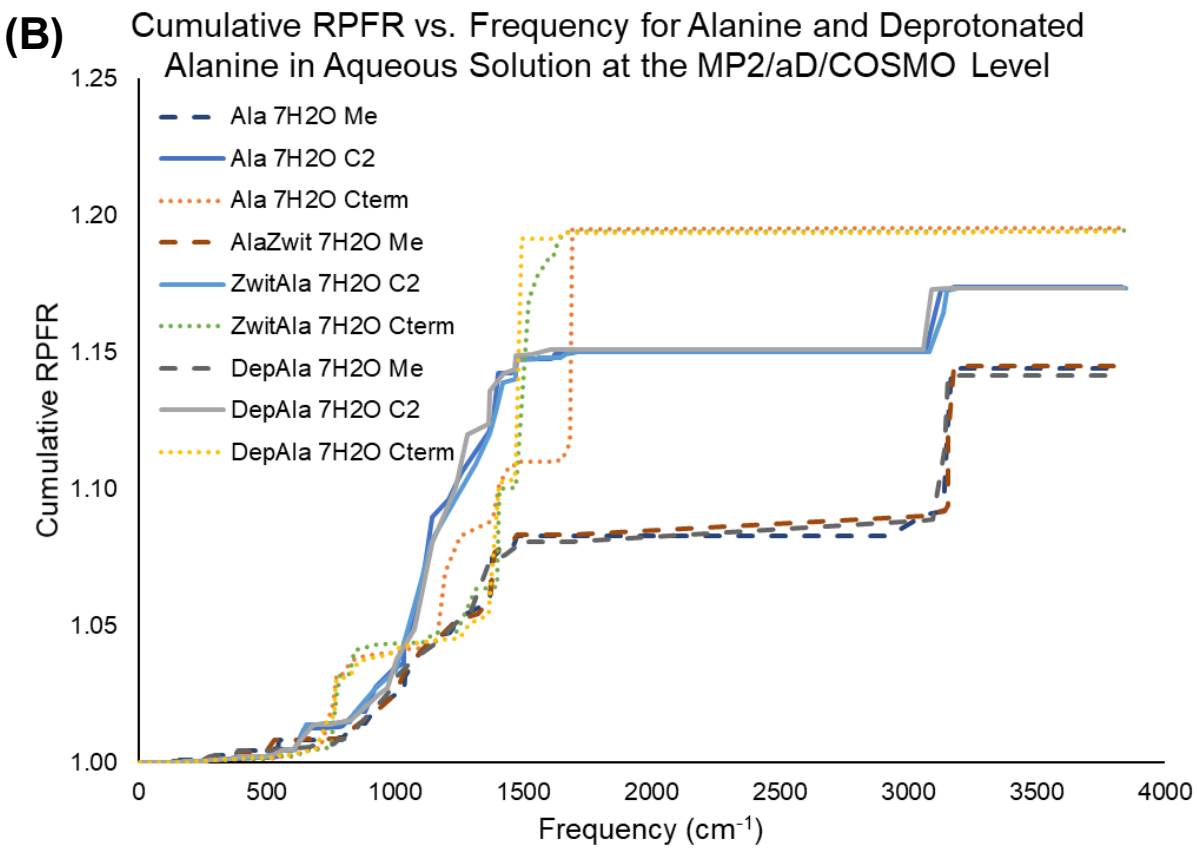
(B)
Cumulative RPFR vs. Frequency for Alanine and Deprotonated Alanine in Aqueous Solution at the MP2/aD/COSMO Level
Ala 7H2O Me
Ala 7H2O C2
Ala 7H2O Cterm
AlaZwit 7H2O Me
ZwitAla 7H2O C2
ZwitAla 7H2O Cterm
DepAla 7H2O Me
DepAla 7H2O C2
DepAla 7H2O Cterm
Cumulative RPFR
1.25
1.20
1.15
1.10
1.05
1.00
0
500
1000
1500
2000
2500
3000
3500
4000
Frequency (cm-1)

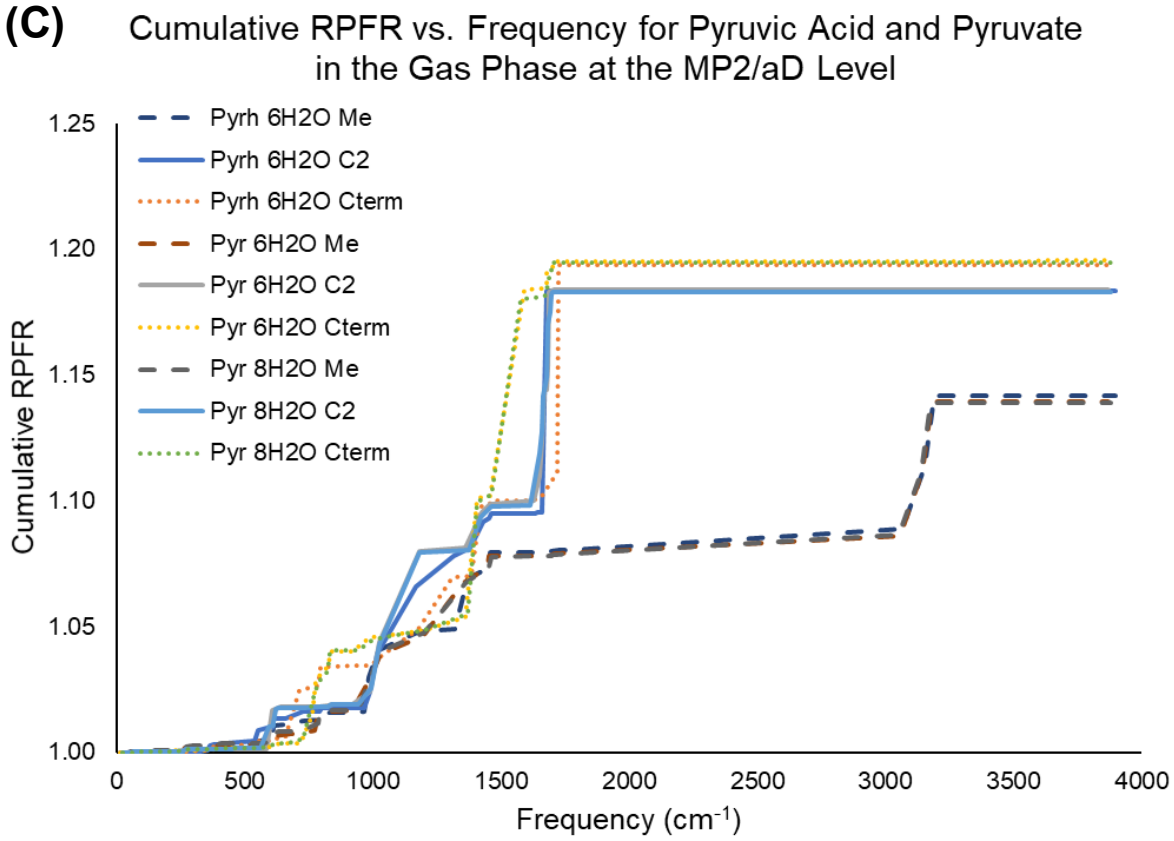
(C)
Cumulative RPFR vs. Frequency for Pyruvic Acid and Pyruvate in the Gas Phase at the MP2/aD Level
Pyrh 6H2O Me
Pyrh 6H2O C2
Pyrh 6H2O Cterm
Pyr 6H2O Me
Pyr 6H2O C2
Pyr 6H2O Cterm
Pyr 8H2O Me
Pyr 8H2O C2
Pyr 8H2O Cterm
Cumulative RPFR
1.25
1.20
1.15
1.10
1.05
1.00
0
500
1000
1500
2000
2500
3000
3500
4000
Frequency (cm-1)

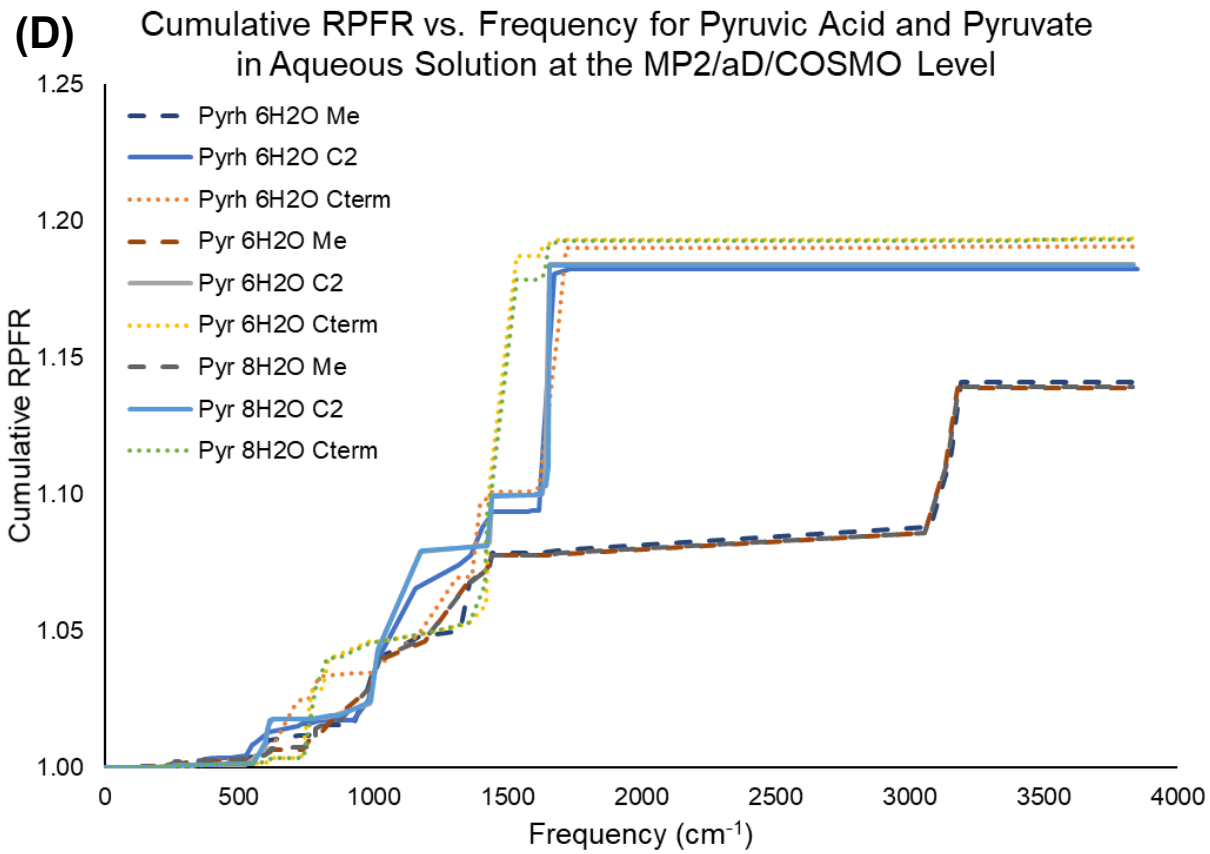

Figure 3. Cumulative reduced partition function ratio (RPFR) vs. vibrational frequency (cm^{-1}) at 298 K for ^{13}C at either the methyl (Me, dashed lines), C2 site (solid lines), or the C-terminus or equivalent (dotted lines). (A) and (B) are alanine in its NCS (Ala) and zwitterionic (ZwitAla) structures and deprotonated alanine (DepAla) with 7 explicit H_2O molecules in the gas phase and in aqueous solution, respectively. (C) and (D) are pyruvic acid (Pyrh) and pyruvate (Pyr) with 6 and 8 explicit H_2O molecules in the gas phase and in aqueous solution, respectively. Pyruvic acid-related results are labeled to correspond to analogous sites in alanine. All results are optimized at the MP2/aD level for the gas phase and MP2/aD/COSMO for the aqueous solution.

Substitution of ^{13}C at the C-terminus site is the most favorable of the substitution sites modeled, as it yields the highest β_{aq} value for all alanine species with 7 explicit H_2O molecules

and ^{13}C substitution at the methyl group is the least favorable (smallest β_{aq}). Analogous values for pyruvic acid species are comparable to those of alanine, as ^{13}C substitution is most favorable at the C-terminus and least favorable at the methyl group. The C2 position for pyruvic acid and pyruvate has a somewhat larger average β_{aq} value (1.1835) than the C2 position of alanine and its various species (average β_{aq} = 1.1742) by 9.3 ‰.

Isotope Fractionation During Aqueous Alanine Transamination. The ALT reaction is catalyzed by the alanine transaminase (ALT) enzyme and involves exchanging the =O at the C2 position of pyruvate with NH_3^+ to form zwitterionic alanine at biological pH in aqueous solution.[46] This reaction was modeled in terms of various components. The free energy of the reaction depends on the enthalpy and entropy which incorporates all of the terms including those due to isotope substitution. This is more complicated than the often-studied isotopic substitution reaction which has a nominal K_{eq} = 1 for all of the same isotopes. Even if one were to just consider the vibrational contributions, the equilibrium constants K_l or K_h with all light or all heavy isotopes are not equal to one. To maintain an equal number of explicit H_2O molecules between reactants and products, pyruvic acid/pyruvate was modeled with 8 explicit H_2O molecules for the isotopic studies.

The aqueous organic reaction between alanine and α-ketoglutarate to form pyruvate and glutamate was modeled in a variety of ways. Equilibrium constants (K) given in Table 4 are calculated from the appropriate Q_l or Q_h values according to the reactions as they are defined in Figure 1. These reactions are also shown with optimized cluster geometries in Figure 4, for which the isotope fractionation factors (ϵ) can be directly compared with the simpler zero-point energy-based approximations (ϵ_{ZPE}), which are described below. A value of K greater than 1 indicates that the reaction equilibrium favors the production of pyruvate and glutamate. In the gas phase, Reactions (1), (3), and (4) are predicted to favor the formation of products, pyruvate and glutamate.

Aqueous Reaction (3), which involves the chemical species as they would appear at biological pH, also slightly favors the formation of products. However, gas phase Reaction (2) and aqueous Reactions (1), (2), and (4) favor the reactants, alanine and α-ketoglutarate. Regardless of the individual equilibrium constant values, the ϵ values (i.e., the change in equilibrium constant on ^{13}C substitution) are in excellent agreement for all four modeled reactions during $^{13}C/^{12}C$ exchange at the C2 site and at the C-terminus. The calculated ϵ values for the C-terminus ^{13}C substitution indicate that the reaction is impeded by this substitution. A heavy carbon at the C-terminus favors the reactants, alanine and α-ketoglutarate, by ~ 1 ‰ in aqueous solution and ~ 3 ‰ in the gas phase. The ϵ for the C2 position ^{13}C substitution predicts that this heavy carbon substitution favors the product, pyruvate, by ~ 9 ‰ in both the gas and aqueous phases. $^{13}C/^{12}C$ substitution at the methyl group is very consistent for Reactions (1), (2), and (4) in both gas and aqueous optimized reactions and favors the reactants by 2.0 to 2.5 ‰. However, methyl substitution differs when the

Table 4. K and ϵ Values for the Reactions of Interest With and Without Heavy Isotopes for Deprotonated Alanine and Pyruvate in the Gas Phase and in Aqueous Solution at 298 K.[a]

Reaction	Opt	K_l	$K_{h,Me}$ [b]	$K_{h,C2}$ [b]	$K_{h,carboxylate}$ [d]	ϵ_{Me} [e]	ϵ_{C2} [e]	$\epsilon_{C\text{-}term}$ [e]
(1)	Gas	1.2149	1.2119	1.2255	1.2110	-2.4747	8.7729	-3.1521
	Aqueous	0.8217	0.8202	0.8291	0.8211	-1.9253	8.9977	-0.7278
(2)	Gas	0.1889	0.1884	0.1905	0.1883	-2.4747	8.7729	-3.1521
	Aqueous	0.3703	0.3696	0.3737	0.3701	-1.9253	8.9977	-0.7278
(3)	Gas	2.8771	2.8631	2.9009	2.8680	-4.8516	8.2957	-3.1348
	Aqueous	1.0220	1.0169	1.0312	1.0212	-4.9791	8.9485	-0.7718
(4)	Gas	1.5423	1.5385	1.5559	1.5375	-2.4747	8.7729	-3.1521
	Aqueous	0.5882	0.5871	0.5935	0.5878	-1.9253	8.9977	-0.7278

[a] Calculation includes Q values for deprotonated alanine with 7 explicit H_2O molecules and pyruvate with 8 explicit H_2O molecules. [b] ^{13}C at the methyl. [c] ^{13}C at the C2 site. [d] ^{13}C at the carboxylate. [e] ϵ values are given in ‰.

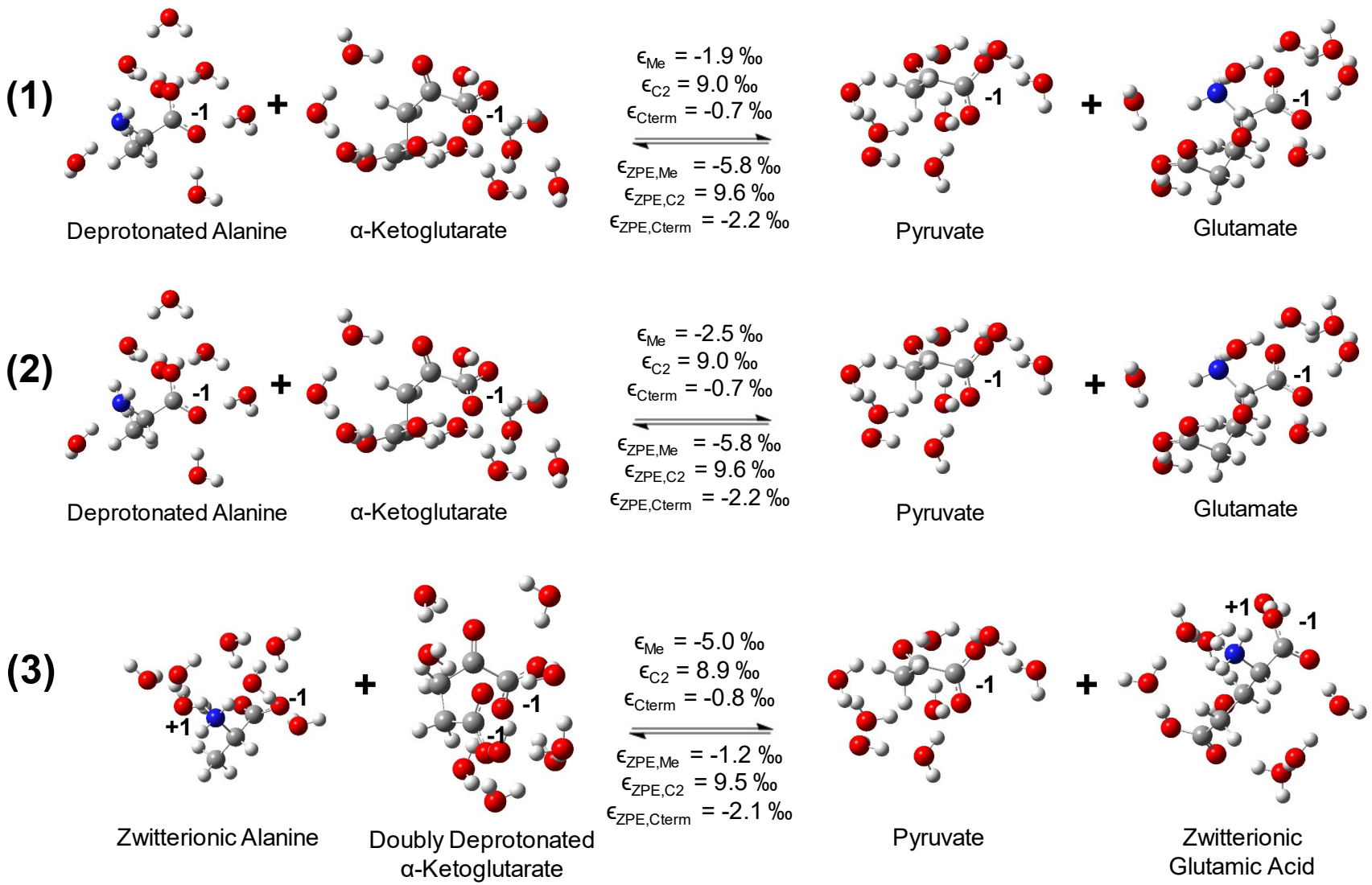
(1)
-1
-1
Deprotonated Alanine
α-Ketoglutarate
ϵ_{Me} = -1.9 ‰
ϵ_{C2} = 9.0 ‰
ϵ_{Cterm} = -0.7 ‰
$\epsilon_{ZPE,Me}$ = -5.8 ‰
$\epsilon_{ZPE,C2}$ = 9.6 ‰
$\epsilon_{ZPE,Cterm}$ = -2.2 ‰
-1
-1
Pyruvate
Glutamate
(2)
-1
-1
Deprotonated Alanine
α-Ketoglutarate
ϵ_{Me} = -2.5 ‰
ϵ_{C2} = 9.0 ‰
ϵ_{Cterm} = -0.7 ‰
$\epsilon_{ZPE,Me}$ = -5.8 ‰
$\epsilon_{ZPE,C2}$ = 9.6 ‰
$\epsilon_{ZPE,Cterm}$ = -2.2 ‰
-1
-1
Pyruvate
Glutamate
(3)
+1
-1
-1
-1
Zwitterionic Alanine
Doubly Deprotonated
α-Ketoglutarate
ϵ_{Me} = -5.0 ‰
ϵ_{C2} = 8.9 ‰
ϵ_{Cterm} = -0.8 ‰
$\epsilon_{ZPE,Me}$ = -1.2 ‰
$\epsilon_{ZPE,C2}$ = 9.5 ‰
$\epsilon_{ZPE,Cterm}$ = -2.1 ‰
-1
+1
-1
Pyruvate
Zwitterionic
Glutamic Acid

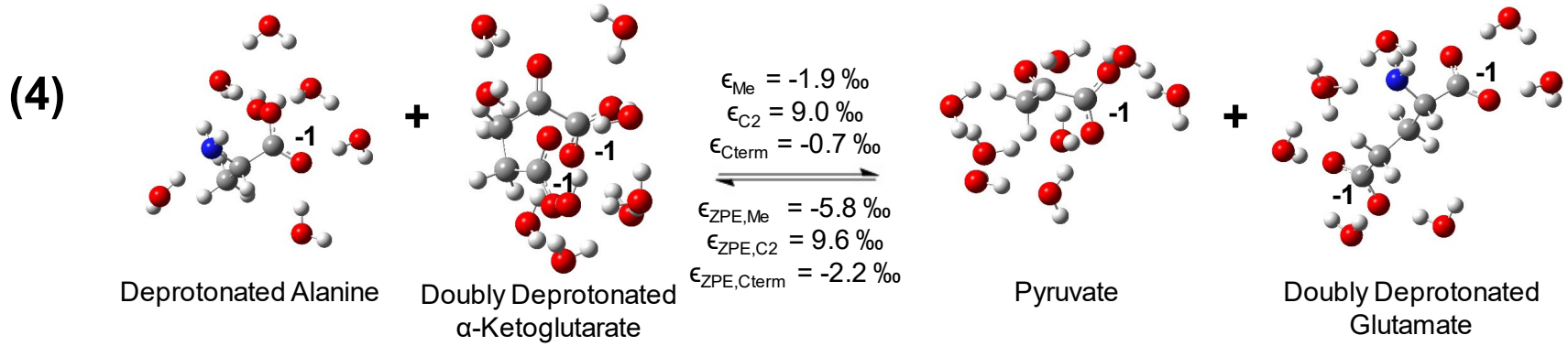

Figure 4. Isotope fractionation factors ϵ and ϵ_{ZPE} at each $^{13}C/^{12}C$ substitution site of alanine and pyruvate for Reactions (1) through (4) with aqueous optimized, explicitly hydrated clusters. Calculated ϵ_{ZPE} values are solely based on the form of alanine and pyruvate in equilibrium with one another.

reaction consists of species present at biological pH (zwitterionic alanine rather than deprotonated alanine) and favors the reactants more strongly by a factor of 2 (4.9 to 5.0 ‰).

Zero-Point Energy-Based Approach. A simpler approach is just to use zero-point energies to estimate ϵ. At T = 0 K, the ϵ values are determined only by changes in the ZPE using Equation 12. ϵ_{ZPE} values shown in Figure 4 for aqueous optimized clusters and are reported in Table S3 for both gas and aqueous optimized clusters for the equilibrium $^{13}C/^{12}C$ exchange reactions between zwitterionic or deprotonated alanine and pyruvate. In both the gas phase and in aqueous solution, ^{13}C substitution at the C2 position of both deprotonated alanine and pyruvate result in favored formation of the heavy product, pyruvate, by 9.2 and 9.5 ‰ in the gas and aqueous optimized reactions, respectively, which is in excellent agreement with the ϵ results of 8.9 to 9.0 ‰. However, $^{13}C/^{12}C$ exchange at the C-terminus favors the heavy reactant, deprotonated alanine, by 4.3 ‰ in the gas phase and 2.1 ‰ in aqueous solution, which is in good agreement with the predicted ϵ of ~ 1 ‰ in aqueous solution and ~ 3 ‰ in the gas phase. The ϵ_{ZPE} values for biological conditions (zwitterionic alanine) are in excellent agreement with the values calculated for $^{13}C/^{12}C$ substitution of deprotonated alanine and pyruvate at the C2 and C-terminus positions. The only exception is that the gas phase optimized ^{13}C substitution of zwitterionic alanine and pyruvate is predicted to favor the formation of heavy pyruvate slightly less ($\epsilon_{ZPE,gas}$ = 7.8 ‰) than the exchange when both species are deprotonated ($\epsilon_{ZPE,aq}$ = 9.2 ‰). $^{13}C/^{12}C$ exchange between the methyl groups of alanine and pyruvate depend much more on the form of species in equilibrium. $^{13}C/^{12}C$ exchange at the methyl group favors zwitterionic alanine over pyruvate by 6.5 ‰ in the gas optimized equilibrium and 5.8 ‰ in the aqueous optimized equilibrium, which is in good agreement with ϵ = 4.9 to 5.0 ‰. Deprotonated alanine is favored over pyruvate, though to a much lesser extent, with a predicted

$^{13}C/^{12}C$ substitution of 1.1 to 1.2 ‰ for both the gas and aqueous optimized reactions, which is also in good agreement with ϵ = 2.0 to 2.5 ‰.

An even simpler estimate to obtain ϵ is to exclude the explicit waters of solvation. ^{13}C exchange between pyruvate and alanine were studied as shown in Reactions (14) and (15) (Figure 5). Vibrational frequencies at a variety of computational levels were used to calculate the IFFs of these reactions from both the zero-point energy-based ϵ_{ZPE} and the more exact ϵ approaches described above, shown in Table 5. For the isotope fractionation equilibria between deprotonated alanine and pyruvate, NCS neutral alanine and pyruvate, and protonated alanine and pyruvic acid in Reactions (14) and (15) with ^{13}C at the C2 position, both ϵ_{ZPE} and ϵ are positive, so ^{13}C will be enriched in the product (pyruvate or pyruvic acid) preferentially over the reactant (NCS alanine or deprotonated alanine). This preference is largest for Reaction (14) and is smallest for Reaction (15).

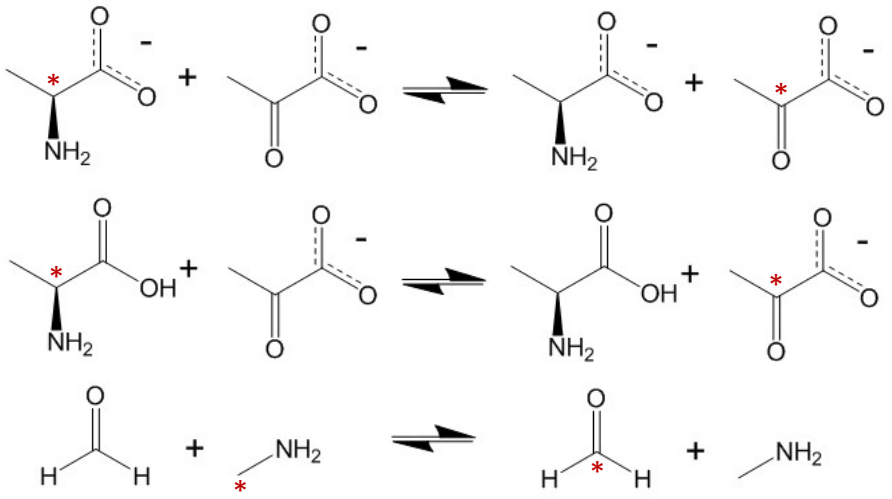

(14)

(15)

(16)

Figure 5. ^{13}C exchange between (14) deprotonated alanine and pyruvate, (15) neutral non-charge separated (NCS) alanine and pyruvate, and (16) formaldehyde (H_2CO) and methylamine (CH_3NH_2). The red asterisk indicates the location of the heavy carbon.

Table 5. Gas Phase Isotope Exchange Values at 298 K at Various Computational Levels in kcal/mol.

	B3LYP/ 6-311++ G(2d,2p) [a]	LSDA/ 6-311++ G(2d,2p) [a]	BP86/ 6-311++ G(2d,2p) [a]	B3LYP/ DZVP2 [b]	LSDA/ DZVP2 [b]	BP86/ DZVP2 [b]	MP2/aD [b]	MP2/aT [b]	MP2/aT [a]
Reaction (14)									
Pyruvate ΔZPE				0.1513	0.1501	0.1445	0.1520	0.1513	
Deprotonated Alanine ΔZPE				0.1435	0.1441	0.1380	0.1447	0.1452	
ΔΔZPE				-0.00779	-0.00600	-0.00645	-0.00736	-0.00618	
ϵ_{ZPE} (‰)				15.6	14.3	14.8	13.3	11.0	
ϵ (‰)				11.9	9.3	9.7	11.2	9.4	
Reaction (15)									
Pyruvate ΔZPE	0.1497	0.1480	0.1428	0.1513	0.1501	0.1445	0.1520	0.1513	
Alanine ΔZPE	0.1439	0.1436	0.1387	0.1477	0.1479	0.1424	0.1498	0.1501	
ΔΔZPE	-0.0058	-0.0044	-0.0041	-0.0036	-0.0022	-0.0021	-0.0022	-0.0012	
ϵ_{ZPE} (‰)	9.4	7.2	6.7	6.1	3.7	3.5	3.7	2.1	
ϵ (‰)				5.3	3.3	2.9	3.1	1.5	
Reaction (16)									
Formaldehyde ΔZPE	0.1119	0.1096	0.1082	0.1121	0.1103	0.1082	0.1099	0.1109	0.1110
Methylamine ΔZPE	0.1058	0.1044	0.1031	0.1068	0.1060	0.1037	0.1076	0.1082	0.1083
ΔΔZPE	-0.0061	-0.0052	-0.0051	-0.0053	-0.0043	-0.0045	-0.0023	-0.0027	-0.0027
ϵ_{ZPE} (‰)	9.8	8.4	8.4	10.4	7.0	8.2	3.9	4.6	4.4
ϵ (‰)	12.6	11.5		13.0	10.2	10.8	7.0	7.7	7.4

[a] Calculated using NWChem (ref 10). [b] Calculated using Gaussian 16 (ref 39).

Table 6 gives ^{13}C site specific β values for gas phase optimized NCS alanine, deprotonated alanine, pyruvic acid, and pyruvate with no explicit H_2O molecules at the MP2/aT level. Analogous values for these compounds at the MP2/aD level are in the Supporting Information. The carboxylic acid site is predicted to be the most favorable for ^{13}C substitution for alanine and pyruvic acid and their various species as these sites yield the largest β values. MP2/aT β values are very similar to those calculated at the MP2/aD level with each MP2/aT value being slightly larger in magnitude than the analogous MP2/aD value. These site specific β values for pyruvic acid and alanine species are in good agreement with the explicitly solvated results for the same species as listed in Table S3, therefore the inclusion of solvent is not necessary for calculating accurate β values for this reaction. Our values for $^{13}C/^{12}C$ substitution in Table 6, when compared with the β value for CO_2 (1.1939) calculated at the MP2/aT level are -43.9 ‰ at the methyl, -14.1 ‰ at the C2 site, and 6.2 ‰ at the carboxylic acid. These values are in good agreement within 2 ‰ with previous literature values for the gas phase zwitterionic structure of alanine calculated at the same MP2/aT level.[47] Note that Rustad[47] has calculated isotopic enrichments in all of the gas phase zwitterionic amino acids relative to CO_2 at the MP2/aD level.

An even simpler model is to look at the isotope exchange between formaldehyde and methylamine as shown in Reaction (16) (Figure 5). Formaldehyde and methylamine serve as a simplified version of the type of exchange that takes place at the C2 sites of pyruvate and alanine. The calculations for Reaction (16) were done at the MP2/aT level given above. For the isotope fractionation equilibrium between formaldehyde and methylamine as written in Reaction (16), both measures of preference for ^{13}C enrichment, ϵ_{ZPE} and ϵ, are positive, so the product containing heavy carbon ($H_2{}^{13}C(O)$) is preferred over the formation of the reactant containing heavy carbon ($H_3{}^{13}CNH_2$).

Table 6. Site Specific β Values for Non-Solvated H_2CO, CH_3NH_2, $CH_3NH_3^+$, Alanine, Deprotonated Alanine, Protonated Alanine, Pyruvic Acid, and Pyruvate in the Gas Phase at 298 K at the MP2/aT Level.

	$\beta = Q_h/Q_l$		
H_2CO	1.1523		
CH_3NH_2	1.1435		
$CH_3NH_3^+$	1.1427		
	^{13}C Methyl	^{13}C Central Carbon	^{13}C COOH/COO^-
Alanine	1.1414	1.1771	1.2013
Deprotonated Alanine	1.1422	1.1677	1.1928
Pyruvic Acid	1.1416	1.1825	1.1929
Pyruvate	1.1363	1.1802	1.1922

For each of the compounds in Table 6, the relationship between cumulative β and frequency is given in Figure 6. This plot demonstrates the frequencies that significantly contribute to the β for each ^{13}C substituted species and ultimately result in pyruvate and formaldehyde being favored for ^{13}C enrichment over alanine and methylamine, respectively. Pyruvate and alanine species shown have ^{13}C at their C2 positions so that formaldehyde and methylamine can be directly compared. Pyruvic acid, and pyruvate, and formaldehyde have C=O stretch frequencies of ~ 1700 cm^{-1} that contribute significantly to the overall β for these molecules. Additionally, pyruvate and, to a slightly lesser extent, pyruvic acid have a frequency of ~ 1150 cm^{-1} (a coupled C-C with C-H or coupled C-C with C-H and O-H) that also increases their β values, which formaldehyde lacks. The cumulative β values of the other analogous molecules that lack the C=O stretch contribution never can catch up, despite having noteworthy increases in β due to significant C-H stretch contributions from frequencies of ~ 3000 to 3200 cm^{-1}. Alanine and methylamine have a set of frequencies from approximately 1000 cm^{-1} to 1600 cm^{-1} that coincide with C-N and the N-H stretches, which contribute significantly more to the β values of alanine compounds than those of methylamine.

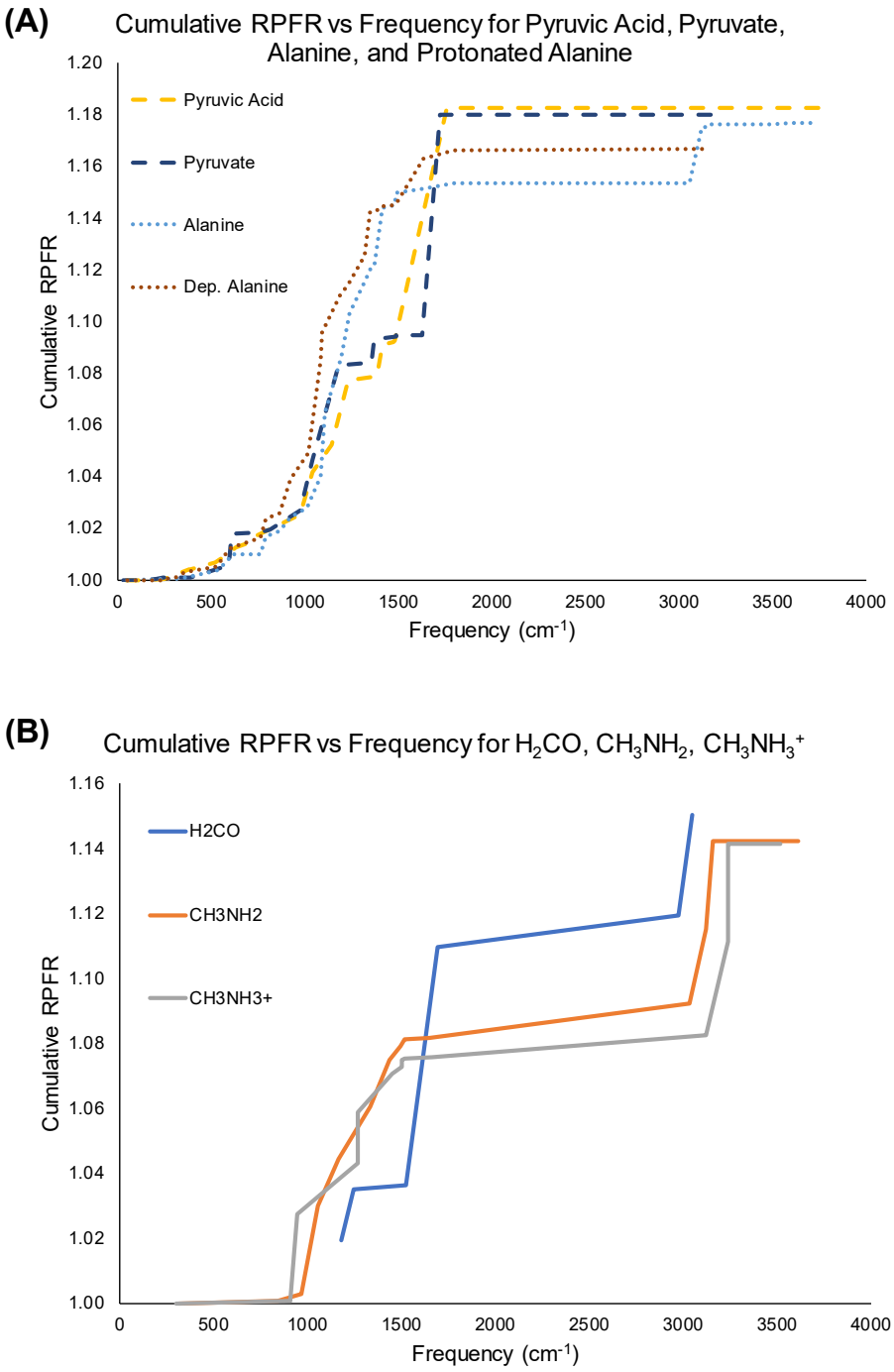

Figure 6. Cumulative reduced partition function ratio (RPFR) vs frequency in cm^{-1} for formaldehyde, methylamine, protonated methylamine, pyruvic acid, pyruvate, alanine, and deprotonated alanine in the gas phase at 298 K. All pyruvate and alanine species are ^{13}C-substituted at the C2 position.

Estimate of ϵ Using Canonical Functional Group Frequencies. As described above, the simple estimate of ϵ for the enrichment of ^{13}C in $R_2C{=}O$ relative to $R_2CH\text{-}NH_2$ gave results within 2 ‰ for the actual ALT reaction. An even simpler approach to predict the isotope fractionation factor ϵ_{ZPE} is to use canonical functional group frequencies rather than frequencies calculated or measured for particular molecules. To estimate how much ^{13}C enrichment one would expect in $R_2C{=}O$ vs $R_2CH\text{-}NH_2$, the system can be approximated in terms of three key frequencies,[48] the carbonyl C=O stretch, the amine C-N stretch, and the C-H stretch in the amine. The canonical group frequencies are given in Table 7. To simplify the analysis, we assume that these canonical group frequencies are associated with the most abundant isotopes; $^{12}C{=}^{16}O$, $^{12}C\text{-}^{14}N$, and $^{12}C\text{-}^{1}H$. Here we use cardinal masses instead of exact masses, due to the inexact nature of using canonical group, as opposed to measured or calculated, frequencies. The isotopically substituted frequency only depends only on the ratio of the reduced masses so we can readily estimate the frequency of the $^{13}C{=}^{16}O$, $^{13}C\text{-}^{14}N$, and $^{13}C\text{-}^{1}H$ vibrations as $\omega_{13}= \sqrt{\frac{\mu_{R12}}{\mu_{R13}}}\,\omega_{12}$. The heavy C frequencies estimated in this way are also given in Table 7.

Table 7. Estimated Reduced Masses and Frequencies for ^{12}C and ^{13}C Bonds with N, O, and H.

	ω_{12} (cm^{-1})	ω_{13} (cm^{-1})
$^{12/13}C\text{-}^{14}N$	1100	1076.98
$^{12/13}C{=}^{16}O$	1750	1711.11
$^{12/13}C\text{-}^{1}H$	3000	2991.11

The free energy of a quantum harmonic oscillator is given by[49]

$$A = \Sigma_i\{½hc\omega_i + k_bT\ln(1 - e^{-hc\omega_i/k_bT})\} \quad (18)$$

in which the first term is the zero-point energy contribution and the second term is the thermal energy contribution to the overall free energy. For the isotope exchange reaction,

$$^{13}C{=}O + {}^{12}CHNH_2 \leftrightarrow {}^{12}C{=}O + {}^{13}CHNH_2 \quad (19)$$

the vibrational free energy change ΔA can be calculated from Equation (18) summed over the three frequencies for the reactants and products; then K is calculated as $e^{-\Delta A/RT}$. Table 8 gives results at T = 298 K so that these values can be compared directly to other values in this work. Analogous values at T = 310 K (37 °C) are given in the SI, which is the temperature relevant for biological systems in warm-blooded mammals. This difference in temperature makes virtually no difference in the ϵ_{ZPE} reported in Table 8. Additionally, the thermal contributions beyond the ZPE are less than 1 ‰ and therefore are not significant to the overall energy of the reaction. Note that K is slightly less than 1 for the reaction as written in Equation 19 as the ^{13}C prefers the stronger bonding environment in the carbonyl bond. Although this very rough model is not in quantitative agreement with our more sophisticated models (too large by a factor of approximately 2), it is qualitatively correct in predicting ^{13}C enrichment in the carbonyl bond.

Table 8. Estimated Free Energy (A), ΔA, and ϵ_{ZPE} in kcal/mol for ^{12}C and ^{13}C Bonds with N, O, and H in kcal/mol at 298 K.

	A ^{12}C			A ^{13}C		
	ZPE	Thermal	Total	ZPE	Thermal	Total
C-N	1.57	-2.92×10^{-3}	1.57	1.54	-3.27×10^{-3}	1.54
C=O	2.50	-1.26×10^{-4}	2.50	2.45	-1.52×10^{-4}	2.45
C-H	4.29	-3.01×10^{-7}	4.29	4.28	-3.14×10^{-7}	4.28
	$^{12}C{=}O + {}^{13}CHNH_2 \leftrightarrows {}^{13}C{=}O + {}^{12}CHNH_2$					
	ΔA	K	ϵ_{ZPE} (‰)			
ZPE + Therm	-9.67×10^{-3}	-0.9844	15.7			
ZPE Only	-9.98×10^{-3}	-0.9839	16.2			

Conclusions

The alanine transaminase (ALT) enzyme catalyzes the reversible transfer of an amino group from alanine to α-ketoglutarate to produce pyruvate and glutamate. As one would expect based on the relative strength of the >C=O bond vs that of the ≡C-NH_2 bond,[4] all levels of calculated models represented in this work predict that ^{13}C will be enriched at the C2 position of pyruvate (>C=O) over the C2 position of alanine (≡C-NH_2). The calculated aqueous free energies for the ALT reaction with explicit and implicit solvation, -3.9 and 3.8 kcal/mol for gas phase and aqueous optimized reactions, respectively, are in decent agreement with the experimental value of 0.25 kcal/mol.[8] The deviation from experiment is due to the limitations of implicit solvation approaches for dianions even with inclusion of explicit solvating water molecules. Isotope fractionation factors (IFFs) for this reaction were calculated from the partition functions of explicitly and/or implicitly solvated alanine, pyruvic acid, glutamic acid, α-ketoglutaric acid, and their various species, which predict a 9.0 ‰ enrichment of ^{13}C in pyruvate over alanine. The computational results are not dependent on whether gas phase or aqueous optimized clusters with and without explicit H_2O molecules were included with the implicit COSMO SCRF approach. Values derived solely from zero-point energy (ZPE) contributions are in excellent agreement with the results including all vibrational components, showing that thermal corrections have virtually no effect on ϵ for this reaction. The inclusion of explicit H_2O molecules does not significantly contribute to the magnitude of the calculated IFFs. In addition to the $^{13}C/^{12}C$ equilibrium between pyruvic acid and alanine or their various species, ZPE-based IFFs (ϵ_{ZPE}) were also calculated using simpler analogues of the molecules of interest, formaldehyde and methylamine. An enrichment in formaldehyde of 7 to 8 ‰ at the MP2/aug-cc-pVDZ and aug-cc-pVTZ levels was predicted to be consistent with the value for the more complex models of the reactants and products. Empirical

estimates based solely on typical values for relevant vibrational modes and reduced masses for C=O, C-H, and C-N produce a qualitative prediction for C=O enrichment over C-N that agrees with the more sophisticated models. In combination with the prior work of Rustad,[47] the computational methods developed here can be used to explore the $^{13}C/^{12}C$ isotopic fractionation of the formation of terrestrial amino acids and extraterrestrial amino acids such as those discovered on meteorites[50,51,52] to further our understanding of the nature of how amino acids are formed in different environments.

Acknowledgements This work was supported by the U.S. Department of Energy (DOE), Office of Science, Office of Basic Energy Sciences (BES), Chemical Sciences, Geosciences, and Biosciences Division through its Geosciences program at Pacific Northwest National Laboratory (PNNL) by a subcontract to The University of Alabama. D. A. Dixon thanks the Robert Ramsay Fund of The University of Alabama for partial support. This research used computational resources of the National Energy Research Scientific Computing Center (NERSC), a User Facility supported by the Office of Science of the U.S. DOE under Contract No. DE-AC02-05CH11231. We wish to thank for support from the NERSC NESAP program for helping improve the performance of NWChem software on their machines. A portion of this research was performed using EMSL, a U.S. DOE Office of Science User Facility sponsored by the Office of Biological and Environmental Research, DE-AC06-76RLO 1830.

Supporting Information Complete citation for reference 39. QM/MM parameters and additional data. Discussion of β values for glutamic acid and α-ketoglutaric acid. Gas phase and aqueous optimized Cartesian (x, y, z) coordinates.

References

[1] Karmen, A.; Wróblewski, F.; LaDue, J. S. Transaminase Activity in Human Blood. *J. Clin. Invest.* **1955**, *34*, 126-133.

[2] Lala, V.; Minter, D. A. *Liver Function Tests*. StatPearls Publishing: Treasure Island, FL, 2019.

[3] Liu, Z.; Que, S.; Zu, J.; Peng, T. Alanine Aminotransferase – Old Biomarker and New Concept: A Review. *Int. J. Med. Sci.* **2014**, *11*, 925-935.

[4] Luo, Y.-R. *Comprehensive Handbook of Chemical Bond Energies*, CRC Press, Taylor and Francis Group, 2007.

[5] Krebs, H. A. Equilibria in Transamination Systems. *Biochem. J.* **1953**, *54*, 82-86.

[6] Segal, H. L.; Beattie, D. S.; Hopper, S. Purification and Properties of Liver Glutamic-Alanine Transaminase from Normal and Corticoid-Treated Rats. *J. Biol. Chem.* **1962**, *237*, 1914-1920.

[7] Martinez-Carrion, M.; Jenkins, W. T. D-Alanine-D-Glutamate Transaminase. I. Purification and Characterization. *J. Biol. Chem.* **1965**, *240*, 3538-3551.

[8] Miller, S. L.; Smith-Magowan, D. The Thermodynamics of the Krebs Cycle and Related Compounds. *J. Phys. Chem. Ref. Data* **1990**, *19*, 1049-1073.

[9] Car, R.; Parrinello, M. Unified Approach to Molecular Dynamics and Density-Functional Theory. *Phys. Rev. Lett*. **1985**, *55*, 2471-2474.

[10] Valiev, M.; Bylaska, E. J.; Govind, N.; Kowalski, K.; Straatsma, T. P.; Van Dam, H. J. J.; Wang, D.; Nieplocha, J.; Apra, E.; Windus, T. L.; et al. NWChem: A Comprehensive and Scalable Open-Source Solution for Large Scale Molecular Simulations. *Comput. Phys. Commun*. **2010**, *181*, 1477-1489.

[11] Bylaska, E. J.; Tsemekhman, K.; Govind, N.; Valiev, M. Large-Scale Plane-Wave-Based Density Functional Theory: Formalism, Parallelization, and Applications. In *Computational*

Methods for Large Systems: Electronic Structure Approaches for Biotechnology and Nanotechnology. Reimers, J. R., Ed.; John Wiley and Sons: Hoboken, NJ, 2011; pp. 77-116.

[12] Bylaska, E. J. Plane-Wave DFT Methods for Chemistry. In *Annual Reports in Computational Chemistry*. Vol. 13, Elsevier, Amsterdam, 2017 Ch. 5, pp. 185-228.

[13] Hohenberg, P.; Kohn, W. Inhomogeneous Electron Gas. *Phys. Rev.* **1964**, *136,* B864-B871.

[14] Kohn, W.; Sham, L. J. Self-Consistent Equations Including Exchange and Correlation Effects. *Phys. Rev.*, **1965**, *140*, A1133-A1138.

[15] Cauët, E.; Bogatko, S.; Weare, J. H.; Fulton, J. L.; Schenter, G. K.; Bylaska, E. J. Structure and Dynamics of the Hydration Shells of the Zn^{2+} Ion from Ab Initio Molecular Dynamics and Combined Ab Initio and Classical Molecular Dynamics Simulations. *J. Chem. Phys*. **2010**, *132*, 194502-1 – 194502-13.

[16] Perdew, J. P.; Burke, K.; Ernzerhof, M. Generalized Gradient Approximation Made Simple. *Phys. Rev. Lett*. **1996**, *77*, 3865-3868.

[17] Hamann, D. R.; Schlüter, M.; Chiang, C. Norm-Conserving Pseudopotentials. *Phys. Rev. Lett.* **1979**, *43*, 1494-1497.

[18] Hamann, D. R. Generalized Norm-Conserving Pseudopotentials. *Phys. Rev. B* **1989**, *40*, 2980-2987.

[19] Kleinman, L.; Bylander, D. M. Efficacious Form for Model Pseudopotentials. *Phys. Rev. Lett*. **1982**, *48*, 1425-1428.

[20] Nosé, S. A Molecular Dynamics Method for Simulations in the Canonical Ensemble. *Mol. Phys*. **1984**, *52*, 255-268.

[21] Hoover, W. G. Canonical Dynamics: Equilibrium Phase-Space Distributions. *Phys. Rev*. **1985**, *31*, 1695-1697.

[22] Blöchl, P. E.; Parrinello, M. Adiabaticity in First-Principles Molecular Dynamics. *Phys. Rev. B* **1992**, *45*, 9413-9416.

[23] Shrake, A.; Rupley, J. A. Environment and Exposure to Solvent of Protein Atoms. Lysozyme and Insulin. *J. Mol. Biol*. **1973**, *79*, 351-371.

[24] Berendsen, H. J. C.; Grigera, J. R.; Straatsma, T. P. The Missing Term in Effective Pair Potentials. *J. Phys. Chem.* **1987**, *91*, 6269-6271.

[25] Environmental Molecular Sciences Laboratory. EMSL Arrows 2D Molecular and Reaction Editor. https://arrows.emsl.pnnl.gov/api/ (accessed Mar 11, 2018).

[26] Stillinger, F. H.; Weber, T. A. Inherent Structure Theory of Liquids in the Hard-Sphere Limit. *J. Chem. Phys.* **1985**, *83*, 4767-4775.

[27] Becke, A. D. Density-Functional Thermochemistry. III. The Role of Exact Exchange. *J. Chem. Phys.* **1993**, *98*, 5648-5652.

[28] Lee, C.; Yang, W.; Parr, R. G. Accurate and Simple Analytic Representation of the Electron-Gas Correlation Energy. *Physical Review B.* **1988**, *37*, 785-789.

[29] Godbout, N.; Salahub, D. R.; Andzelm, J.; Wimmer, E. Optimization of Gaussian-Type Basis-Sets for Local Spin-Density Functionals Calculations. 1. Boron Through Neon, Optimization Technique and Validation. *Can. J. Chem.* **1992**, *70*, 560-571.

[30] Møller, C.; Plesset, M. S. Note on an Approximation Treatment for Many-Electron Systems. *Phys. Rev.* **1934**, *46*, 0618-0622.

[31] Pople, J. A.; Binkley, J. S.; Seeger, R. Theoretical Models Incorporating Electron Correlation. *Int. J. Quantum. Chem.* **1976**, *10*, 1-19.

[32] Dunning, T. H., Jr. Gaussian Basis Sets for Use in Correlated Molecular Calculations. I. The Atoms Boron Through Neon and Hydrogen. *J. Chem. Phys*. **1989**, *90*, 1007-1023.

[33] Kendall, R. A.; Dunning, T. H. Jr.; Harrison, R. J., Electron Affinities of the First Row Atoms Revisited. Systematic Basis Sets and Wave Functions. *J. Chem. Phys*. **1992,** *96*, 6796-6806.

[34] Tomasi, J.; Mennucci, B.; Cammi, R. Quantum Mechanical Contiuum Solvation Models. *Chem. Rev.* **2005**, 105, 2999-3093.

[35] Klamt, A. *Quantum Chemistry to Fluid Phase Thermodynamics and Drug Design*. Elsevier: Amsterdam, 2005.

[36] Klamt, A.; Schüürmann, G. J. COSMO: A New Approach to Dielectric Screening in Solvents with Explicit Expressions for the Screening Energy and Its Gradient. *Chem. Soc. Perkin Trans.* **1993**, 2, 799-805.

[37] Feyereisen, M. W.; Feller, D.; Dixon, D. A. The Hydrogen Bond Energy of the Water Dimer. *J. Phys. Chem*. **1996**, *100*, 2993-2997

[38] Rustad, J. R.; Nelmes, S. L.; Jackson, V. E.; Dixon, D. A. Quantum-Chemical Calculations of Carbon-Isotope Fractionation in CO_2(g), Aqueous Carbonate Species, and Carbonate Minerals. *J. Phys. Chem. A*, **2008**, *112*, 542-555.

[39] Gaussian 16, Revision E.01, Frisch, M. J.; Trucks, G. W.; Schlegel, H. B.; Scuseria, G. E.; Robb, M. A.; Cheeseman, J. R.; Montgomery, Jr., J. A.; Vreven, T.; Kudin, K. N.; Burant, J. C.; et al., Gaussian, Inc., Wallingford CT, 2004.

[40] Slater, J. C. *The Self-Consistent Field for Molecular and Solids*, *Quantum Theory of Molecular and Solids.* McGraw-Hill: New York, 1974; Vol. 4.

[41] Vosko, S. H.; Wilk, L.; Nusair, M. Accurate Spin-Dependent Electron Liquid Correlation Energies for Local Spin Density Calculations: A Critical Analysis. *Can. J. Phys.* **1980**, *58*, 1200-1211.

[42] Perdew, J. P. Density-Functional Approximation for the Correlation Energy of the Inhomogeneous Electron Gas. *Phys. Rev. B* **1986**, *33*, 8822-8824.

[43] Becke, A. D. Density-Functional Exchange-Energy Approximation with Correct Asymptotic Behavior. *Phys. Rev. A* **1988**, *88*, 3098-3100.

[44] Ditchfield, R.; Hehre, W. J.; Pople, J. A. Self-Consistent Molecular Orbital Methods. IX. Extended Gaussian-Type Basis for Molecular-Orbital Studies of Organic Molecules. *J. Chem. Phys.* **1971**, *54*, 724-728.

[45] Lide, D. R. (E.) *CRC Handbook of Chemistry and Physics*, 86th Ed. CRC Press, Boca Raton, FL, USA, 2006.

[46] Barb, A. W.; Hekmatyar, S. K.; Glushka, J. N.; Prestegard, J. H. Probing Alanine Transaminase Catalysis with Hyperpolarized $^{13}CD_3$-Pyruvate. *J. Magn. Reson.* **2013**, *228*, 59 – 65.

[47] Rustad, J. R. Ab Initio Calculation of the Carbon Isotope Signatures of Amino Acids. *Org. Geochem.* **2009**, *40*, 720 – 723.

[48] Silverstein, R. M.; Bassler, G. C.; and Morrill, T. C. *Spectrometric Identification of Organic Compounds*, 4th ed. John Wiley and Sons: New York, 1981.

[49] McQuarrie, D. A. *Statistical Mechanics.* University Science Books: Sausalito, CA, 2000.

[50] Glavin, D. P.; Bada, J. L.; Brinton, K. L. F.; McDonald, G. D. Amino Acids in the Martian Meteorite Nakhla. *Proc. Natl. Acad. Sci. USA* **1999**, *96*, 8835-8838.

[51] Koga, T.; Naraoka, H. A New Family of Extraterrestrial Amino Acids in the Murchison Meteorite. *Sci. Rep.* **2017**, *7*, 636-1 – 636-8.

[52] Chan, Q. H. S.; Zolensky, M. E.; Kebukawa, Y.; Fries, M.; Ito, M.; Steele, A.; Rahman, Z.; Nakato, A.; Kilcoyne, A. L. D.; Suga, H.; et al. Organic Matter in Extraterrestrial Water-Bearing Salt Crystals. *Sci. Adv.* **2018**, *4*, eaao3521-1 – eaao3521-10.

TOC Graphic

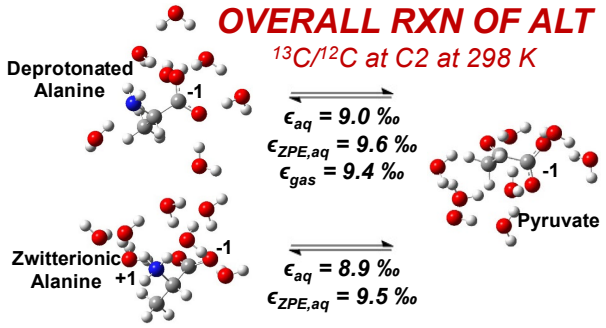
OVERALL RXN OF ALT
$^{13}C/^{12}C$ at C2 at 298 K
Deprotonated Alanine
-1
ϵ_{aq} = 9.0 ‰
$\epsilon_{ZPE,aq}$ = 9.6 ‰
ϵ_{gas} = 9.4 ‰
-1
Pyruvate
Zwitterionic Alanine
+1
-1
ϵ_{aq} = 8.9 ‰
$\epsilon_{ZPE,aq}$ = 9.5 ‰